0026-895X/06/7002-532–541$20.00
MOLECULAR PHARMACOLOGY
Copyright © 2006 The American Society for Pharmacology and Experimental Therapeutics
Mol Pharmacol 70:532–541, 2006

Vol. 70, No. 2
16451/3127805
Printed in U.S.A.

Mammalian Tolloid Alters Subcellular Localization, Internalization, and Signaling of α_{1a}-Adrenergic Receptors[S]

Qi Xu, Ning Xu, Tan Zhang, Hui Zhang, Zijian Li, Feng Yin, Zhizhen Lu, Qide Han, and Youyi Zhang

Institute of Vascular Medicine, Peking University Third Hospital and Key Laboratory of Molecular Cardiovascular Sciences, Ministry of Education, Beijing, China

Received July 4, 2005; accepted May 11, 2006

ABSTRACT

In the present study, we identified the CUB5 domain of mammalian Tolloid (mTLD) as a novel protein binding to α_{1A}-adrenergic receptor (AR) using the yeast two-hybrid system. Whereas CUB5 did not couple to either α_{1B}-AR or α_{1D}-AR. It was determined that amino acids 322 to 359 of α_{1A}-AR were the major binding region for CUB5. The direct interaction between α_{1A}-AR cytoplasmic tail and CUB5 was discovered by glutathione *S*-transferase pull-down assay. We confirmed the interaction of mTLD with α_{1A}-AR in human embryonic kidney (HEK) 293 cells by immunoprecipitation, immunofluorescence, and fluorescence resonance energy transfer. Although mTLD did not affect the density and affinity of receptors in crudely prepared membranes from HEK293 cells stably expressing α_{1A}-AR, it significantly altered the subcellular localization of the receptors. Moreover, mTLD reduced the level of cell surface α_{1A}-ARs, delayed the initial rate of agonist-induced receptor internalization, and facilitated agonist-induced calcium transient. We have demonstrated that mTLD interacts with α_{1A}-AR directly, alters the subcellular localization of receptor, and influences agonist-induced α_{1A}-AR internalization and calcium signaling.

α_1-Adrenergic receptors (ARs) are G-protein-coupled receptors (GPCRs) that respond to norepinephrine and epinephrine. α_1-ARs can be classified into at least three subtypes, termed α_{1A}, α_{1B}, and α_{1D}, according to their ligand specificity and their amino acid sequences. Although the three α_1-AR subtypes all couple to the $G_{q/11}$ signaling pathway, they have distinct functional roles in mediating vascular smooth muscle contraction and cardiomyocyte hypertrophy (Zhu et al., 1997; Autelitano and Woodcock, 1998; Grupp et al., 1998).

As the largest family of membrane proteins, GPCRs respond to extracellular stimulations and convert them to intracellular signals. In general, this transduction is defined as follows: ligand binding changes the conformation of receptor's intracellular region, which induces the interaction of receptor with heterotrimeric G-proteins and the ultimate dissociation of Gα and G$\beta\gamma$ subunits. These activated subunits can stimulate and/or inhibit a variety of intracellular effectors. A large number of intracellular molecules other than G-proteins (non–G-proteins) could also interact with GPCR, mediate the intracellular response, or regulate the receptor's state, distribution, and function (Hall et al., 1999; Heuss and Gerber, 2000; Brzostowski and Kimmel, 2001).

ARs have been shown to associate with several non–G-proteins. The majority of them were identified for β_2-AR, such as βARK, β-arrestin, AKAP79/150, NHERF, and eIF-2B (Klein et al., 1997; Menard et al., 1997; Hall et al., 1998; Fraser et al., 2000; Cong et al., 2001); only a few proteins are reported to interact with α_1-AR. Among them, the μ_2 subunit of the AP2 clathrin adaptor complex specifically interacts with α_{1B}-AR (Diviani et al., 2003), whereas tissue transglutaminase II (G_h) and gC1q-R interact with α_{1B}- and α_{1D}-AR (Chen et al., 1996; Pupo and Minneman, 2003). Neuronal nitric-oxide synthase was believed previously to interact with α_{1A}-AR but was found to interact with all three subtypes of

This work was supported by the National Key Basic Research Program of People's Republic of China (grant G2000056906), the Natural Science Foundation of China (grant 30270540), and The Natural Science Foundation of Beijing (grant 7042033).

[S] The online version of this article (available at http://molpharm.aspetjournals.org) contains supplemental material.

Article, publication date, and citation information can be found at http://molpharm.aspetjournals.org.
doi:10.1124/mol.105.016451.

ABBREVIATIONS: AR, adrenergic receptor; GPCR, G-protein-coupled receptor; mTLD, mammalian Tolloid; FRET, fluorescence resonance energy transfer; GST, glutathione *S*-transferase; PCR, polymerase chain reaction; HA, hemagglutinin; aa, amino acids; AT1R, angiotensin II type 1 receptor; EGFP, enhanced green fluorescent protein; HEK, human embryonic kidney; TRITC, tetramethylrhodamine B isothiocyanate; PBS, phosphate-buffered saline; BE2254, 2-[[2-(4-hydroxy-3-iodo-phenyl)ethylamino]methyl]tetralin-1-one; ELISA, enzyme-linked immunosorbent assay.

α_1-AR and β_1- and β_2-ARs (Pupo and Minneman, 2002). So far, no interacting protein has been identified specifically for α_{1A}-AR, the most important and efficient subtype of α_1-AR (Zhong and Minneman, 1999; Zhong et al., 2001).

CUB5 domain, a segment of mammalian Tolloid (mTLD) (Takahara et al., 1994), has been identified as an α_{1A}-AR coupling protein by our group (Xu et al., 2003). In the present study, we have further explored the interaction of α_{1A}-AR and mTLD. In particular, we investigated the differential interactions of CUB5 domain with three α_1-AR subtypes and the region of α_{1A}-AR that binds to the CUB5 domain. We also assessed this interaction by glutathione *S*-transferase (GST)-α_{1A}-AR fusion protein pull-down assay, immunoprecipitation, immunofluorescence, and fluorescence resonance energy transfer (FRET). Moreover, the effects of mTLD on pharmacological property, localization, and signaling of α_{1A}-AR were also investigated in this study.

Materials and Methods

Plasmid DNAs. Flag-tagged human α_{1A}-, α_{1B}-, and α_{1D}-ARs and C-terminally truncated α_{1A}-ARs in mammalian expression vectors $_{p}$DT-α_{1A}, -α_{1B}, -α_{1D}, and -α_{1A}CT, and the GST-tagged α_{1A}-AR cytoplasmic tail, GST-α_{1A}, were generous gifts from Dr. Kenneth P. Minneman (Department of Pharmacology, Emory University, Atlanta, GA). The cDNA sequence encoding the α_{1B}- and α_{1D}-AR cytoplasmic tail and various fragments of the α_{1A}-AR carboxyl terminus were generated by PCR and cloned into pGBKT7 with EcoRI and BamHI sites (see Supplemental Data). PCR reactions were carried out using high-fidelity *Pfx* DNA polymerase (Invitrogen, Carlsbad, CA).

cDNA encoding human mTLD (P13497) was obtained from Invitrogen. For mammalian cell expression, PCR products were subcloned into pcDNA3.1 (+) with NheI and XhoI sites to generate pMT, and other HA-tagged PCR products were also subcloned into pcDNA3.1 (+) with NheI and PmeI sites to generate pMT/HA (supplemental data). The cDNA of prey 3, which encodes aa 867 to 986 of mTLD, was subcloned into pcDNA3.1 (+) with EcoRI and BamHI sites to generate HA-tagged pcP3HA, as we described previously (Xu et al., 2003). Construct EGFP-α_{1A}, expressing fused EGFP/α_{1A}-AR, was made by cutting α_{1A}-AR cDNA with its flank EcoRI and BamHI restriction sites from $_{p}$DT-α_{1A} and then cloning back into the EGFP-C2 expression vector. All constructs were confirmed with Prism 3700 DNA automatic sequencer (Applied Biosystems Inc., Foster City, CA).

Yeast Two-Hybrid. We used pretransformed MATCHMAKER two-hybrid system (Clontech, Mountain View, CA) to perform the screening. Yeast *Saccharomyces cerevisiae* strains AH109 and Y187 were used as the host for the in vivo interaction studies. Yeast two-hybrid analysis was carried out as described in Clontech's user manual. PGAACT, a bait plasmid containing α_{1A}-AR aa 322 to 466 was transformed into yeast strain AH109 by the LiCl/polyethylene glycol method, and mating with human brain cDNA pretransformed yeast strain Y187. Prey plasmids were isolated from the positive colonies using the Zymoprep Yeast Plasmid Minipreparation Kit (Zymo Research, Orange, CA) and sequenced with Prism 3700 DNA automatic sequencer.

β-Galactosidase activity was used to test interactions between different fusion proteins. In brief, both bait and prey plasmids were transformed into the yeast strain Y187; then, β-galactosidase activities were measured by colony-lift filter assay and liquid β-galactosidase assay with *O*-nitrophenyl glycoside (Merck and Co., Inc., Whitehouse Station, NJ).

GST Pull-Down Assay. MagneGST Pull-Down System (Promega, San Luis Obispo, CA) was used for direct interaction assays between α_{1A}-AR and mTLD. GST-α_{1A}-AR cytoplasmic tail fusion proteins or GST proteins were lysed from 1 ml of bacterial culture, and immobilized on MagneGST Particles. Transcription/translation of aa 867 to 986 of mTLD was undertaken in vitro using TNT T7 Quick-Coupled transcription/translation reactions Master Mix (Promega, Madison, WI). Binding reactions were performed in 200 μl of binding/wash buffer (4.2 mM Na_2HPO_4, 2 mM KH_2PO_4, 140 mM NaCl, and 10 mM KCl, pH 7.2) for 1 h at room temperature. Particles were washed five times with the same buffer, and bound proteins were analyzed by immunoblotting.

Cell Line, Culture, and Transfection. HEK293 cells were obtained from the American Type Culture Collection (Manassas, VA) and cultured in glutamine-containing high-glucose Dulbecco's modified Eagle's medium supplemented with 10% fetal bovine serum, 1 mM sodium pyruvate, 100 mg/ml streptomycin, and 100 U/ml penicillin at 37°C under a 95% air/5% CO_2 atmosphere. HEK293 cells stably transfected $_{p}$DT-α_{1A} were also cultured in the same conditions except that 200 mg/ml G418 (Geneticin) was added. Lipofectamine 2000 (Invitrogen) was used in all transfection experiments.

Coimmunoprecipitation Assay. HEK293 cells were transfected and cultured for 48 h. Immunoprecipitation was performed as described previously (Vazquez-Prado et al., 2000) with minor modifications. In brief, cells were washed with ice-cold PBS and lysed for 1 h on ice in lysis buffer (10 mM Tris-HCl, pH 7.4, 50 mM NaCl, 5 mM EDTA, 1% Triton X-100, and 0.05% SDS) supplemented with 50 mM sodium fluoride, 100 mM sodium orthovanadate, 10 mM sodium pyrophosphate, 20 mg/ml aprotinin, 20 mg/ml leupeptin, and 100 mg/ml phenylmethylsulfonyl fluoride. Cell lysates were centrifuged at 12,700*g* for 15 min, and the supernatants were incubated overnight at 4°C with the anti-Flag M2 affinity resin (Sigma-Aldrich.) or anti-c-myc antibodies (Santa Cruz Biotechnology, Inc., Santa Cruz, CA) plus protein G resin (Sigma-Aldrich). After four washes with lysis buffer without protease inhibitors, the immune complexes were denatured by boiling in 2× loading buffer and analyzed by immunoblotting. Anti-α_{1A}-AR antibodies (Santa Cruz Biotechnology), anti-mTLD antibodies, and Supersignal West Pico Chemiluminent (Pierce Biotechnology, Inc.) were used to detect proteins.

Immunofluorescence and Fluorescence Resonance Energy Transfer. HEK293 cells were plated on glass coverslips and cotrans-

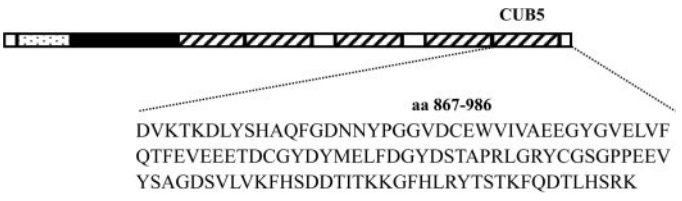

Binding domain fusion construct	Activation domain fusion construct	β-galactosidase activity
PGAACT	prey3	++
PGABCT	prey3	–
PGADCT	prey3	–

Fig. 1. A summary of the interaction between CUB5 and α_{1A}-AR receptor cytoplasmic tail in the yeast two-hybrid system. Top, schematic map of mTLD, with the CUB5 domain shown. A yeast two-hybrid assay identified aa 867 to 986 of mTLD (encompassing the CUB5 domain, aa 865 to 931) as a potential partner for the cytoplasmic tail of α_{1A}-AR. Bottom, colony-lift filter assay (X-Gal) indicates that CUB5 interacts only with the cytoplasmic tail of α_{1A}-AR, not that of α_{1B}-AR and α_{1D}-AR. In this assay, yeast cells transformed with the CUB5 cDNA construct and the PGAACT construct turn blue (++) in 3 h after incubation at 30°C on filters, indicating activation of the reporter gene β-galactosidase. In contrast, yeast cells transformed with CUB5 cDNA constructs and PGABCT/PGADCT remained white after 12 h.

fected with EGFP-α_{1A} and pMT/HA. Twenty-four hours after transfection, cells were fixed in 4% formaldehyde for 10 min and permeated with 0.1% Triton X-100 for 10 min. The fixed cells were incubated with anti-HA monoclonal antibodies (1:100 dilutions; Santa Cruz Biotechnology) overnight at 4°C and then with a TRITC-conjugated anti-mouse antibody (1:200 dilution; Invitrogen) for 1 h. The distributions of α_{1A}-AR and mTLD were examined with a confocal laser-scanning microscope system (TCS SP2; Leica, Wetzlar, Germany) with a 40× oil immersion objective lens. Fluorescence of TRITC was then excited continuously for 5 min to bleach the TRITC signal irreversibly. Images of the EGFP fluorescence were acquired before and after photobleaching. The extent of FRET was assessed by calculating the ratio of the EGFP fluorescence before (D_A) and after (D) photobleaching, using the equation $E = D/D_A$. Nine to ten cells from three individual experiments were selected, and the D/D_A of intracellular areas was averaged.

Radioligand Binding. HEK293 cells stably transfected PDT-α_{1A} were plated in 10-cm dishes and transfected with pcDNA3.1/LacZ or pMT. Forty-eight hours after transfection, cells were washed with PBS, pH 7.6, and harvested. After centrifugation and homogenization with a Polytron homogenizer (Kinematica, Basel, Switzerland), cell membranes were collected by centrifugation at 20,000*g* for 20 min and resuspended in PBS. Radioligand binding sites were measured by saturation analysis of specific binding of the α_{1A}-AR antagonist radioligand ^{125}I-BE2254 (15–500 pM). Nonspecific binding was defined as binding in the presence of phentolamine at 100 μM.

Whole-Cell ELISA. HEK293 cells stably transfected with $_P$DT-α_{1A} were plated in poly-D-lysine–coated 24-well plates and transfected with pcDNA3.1/LacZ or pMT. Forty-eight hours later, cells were incubated with DMEM containing phenylephrine (10 μM) for 0 to 60 min at 37°C. The transfected cells were then fixed in 2% formaldehyde for 10 min without permeating the cells. Changes in surface receptor density were subsequently determined by ELISA, taking advantage of the FLAG-tag in α_{1A}-AR. Cells were labeled with the anti-FLAG M2 antibody (1:1000 dilution; Sigma-Aldrich) followed by anti-mouse antibody (1:1000 dilution; Jackson ImmunoResearch, West Grove, PA). Antibody labeling was detected by incubation with *O*-phenylenediamine (Sigma-Aldrich, Inc.), and absorbance was read at 490 nm.

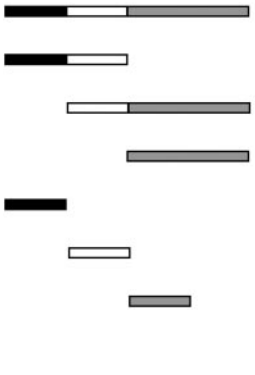

	colony-lift filter assay	Liquid β-galactosidase assay
322-466aa	++	3.07 ± 0.81
322-398aa	+++	5.93 ± 1.43
360-428aa	+	1.21 ± 0.17
399-466aa	+	2.14 ± 0.50
322-359aa	++	3.40 ± 1.35
360-398aa	–	0.13 ± 0.07
399-428aa	+	1.37 ± 0.24
Control	–	0.07 ± 0.03

Fig. 2. Schematic diagram showing the interaction between CUB5 domain with truncated α_{1A}-AR constructs as determined using the yeast two-hybrid assay. A series of deletion truncations of α_{1A}-AR cytoplasmic tail constructs were cotransfected into Y187 with cDNA of the CUB5 domain. Black block, primary biding region; gray block, subsidiary binding region; white, nonbinding region. The interactions were tested using both X-Gal colony-lift filter assay and liquid β-galactosidase assay with *O*-nitrophenyl glycoside. Results from the colony-lift filter assay are classified as follows: +++, turned blue in 1 h after incubation at 30°C on filters; ++, turned blue in 3 h, +, turned blue in 5 h; –, color unchanged after 12 h. In the liquid β-galactosidase assay, results are the mean ± S.E. of four independent experiments.

Intracellular Calcium Measurement. $_P$DT-α_{1A} stably transfected HEK293 cells were transfected with pcDNA3.1/LacZ or pMT. Twenty-four hours after transfection and a further 8 h of serum starvation, cells were loaded with calcium indicator, fluo-4^{AM} (Invitrogen), as described previously (Wang et al., 2001). Fluorescence was visualized by Zeiss LSM510 confocal microscope (Oberkochen, Germany) equipped with an argon laser (488 nm) and 40×, 1.3 numerical aperture oil immersion objective lens. Images were acquired at sampling rates of 10 s/image, and phenylephrine (10 μM) was added after the first three images were acquired. The digital images were analyzed with IDL image-processing software (ver. 5.4; RSI, Boulder, CO). Four to five cells were selected, and the average fluorescence density of intracellular areas was measured to indicate calcium level. All the data were normalized by fluorescent density before stimulation.

Statistical Analysis. All data are presented as means ± S.E. Data obtained from radioligand binding and ELISA assay were analyzed with an unpaired *t* test or analysis of variance (analysis of variance) followed by unpaired *t* test. $P < 0.05$ was considered significant.

Results

mTLD CUB5 Domain Interacts with α_{1A}-AR via Yeast Two-Hybrid Assay. To identify proteins interacting with α_{1A}-AR, we screened a human brain cDNA library, using the yeast two-hybrid assay with the cytoplasmic tail (aa 322–466) of α_{1A}-AR as bait. More than 2×10^7 colonies were screened, and positive colonies were identified by monitoring the activation of reporter genes *HIS3*, *ADE2*, and *MEL1*. Plasmids containing prey cDNA from each positive colony were isolated and sequenced. Of the nine positive colonies obtained, six prey plasmids were identified. As shown in Fig. 1, top, the cDNA of prey 3 encodes aa 867 to 986, the CUB5 domain, of protein mTLD.

We then determined whether CUB5 domain could also interact with other subtypes of α_1-AR in yeast two-hybrid system. We found that only yeast cells transformed with CUB5 cDNA constructs and cytoplasmic tail of α_{1A}-AR cDNA

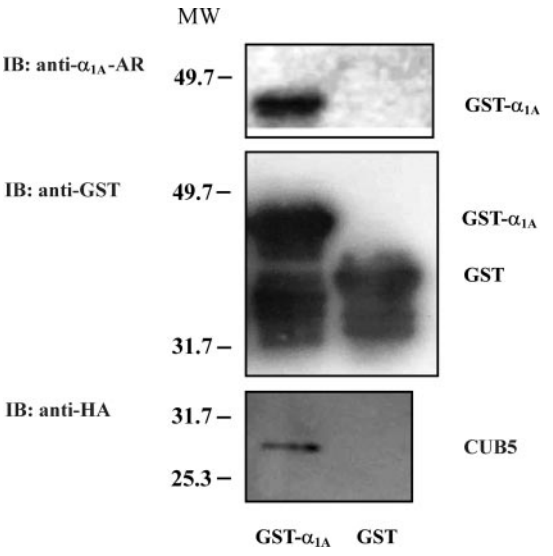

Fig. 3. Direct interaction of the CUB5 domain with α_{1A}-AR cytoplasmic tail. GST or GST-α_{1A}-AR-cytoplasmic-tail fusion proteins were purified from 1 ml of bacterial cultures; HA-tagged CUB5 domains were synthesized in vitro. Then GST or GST-α_{1A}-AR-cytoplasmic-tail fusion proteins (60 μg) and CUB5 domains (60 μg) were added together and subjected to GST pull-down. Bound proteins were analyzed by immunoblotting with anti-α_{1A}-AR antibodies (top), anti-GST (middle), and anti-HA (bottom).

constructs showed an obvious activation of reporter gene β-galactosidase, which was consistent with the yeast two-hybrid assay screening results. No such interaction was detected between the CUB5 domain and cytoplasmic tail of either α_{1B}-AR or α_{1D}-AR (Fig. 1, bottom).

Amino Acid Residues 322 to 359 of α_{1A}-AR Are Important for Interaction with CUB5. As mentioned above, the whole cytoplasmic tail of α_{1A}-AR was used as bait in the yeast two hybrid screen. To localize the CUB5 domain interaction on α_{1A}-AR C terminus, a series of truncations of α_{1A}-AR cytoplasmic tail, illustrated in Fig. 2, were screened against CUB5 domain. Both X-Gal colony-lift filter assay and liquid β-galactosidase assay yielded similar results (Fig. 2). Truncations of the carboxyl end of α_{1A}-AR were quite tolerated, displaying positive interactions with CUB5. Only a small fragment, containing residues 360 to 398, did not interact with CUB5. Truncations from the amino terminus of the α_{1A}-AR cytoplasmic tail narrowed the region for interaction with CUB5 domain to residues 322 to 359.

Association of mTLD with α_{1A}-AR in Vitro and Vivo. To examine whether mTLD can directly interact with α_{1A}-AR, purified GST-α_{1A}-AR-cytoplasmic-tail fusion proteins from bacterial cells and in vitro synthesized CUB5 domains were subject to GST pull-down assay. The bound proteins were fractionated by SDS-polyacrylamide gel electrophoresis and detected by Western blotting. As shown in Fig. 3, the

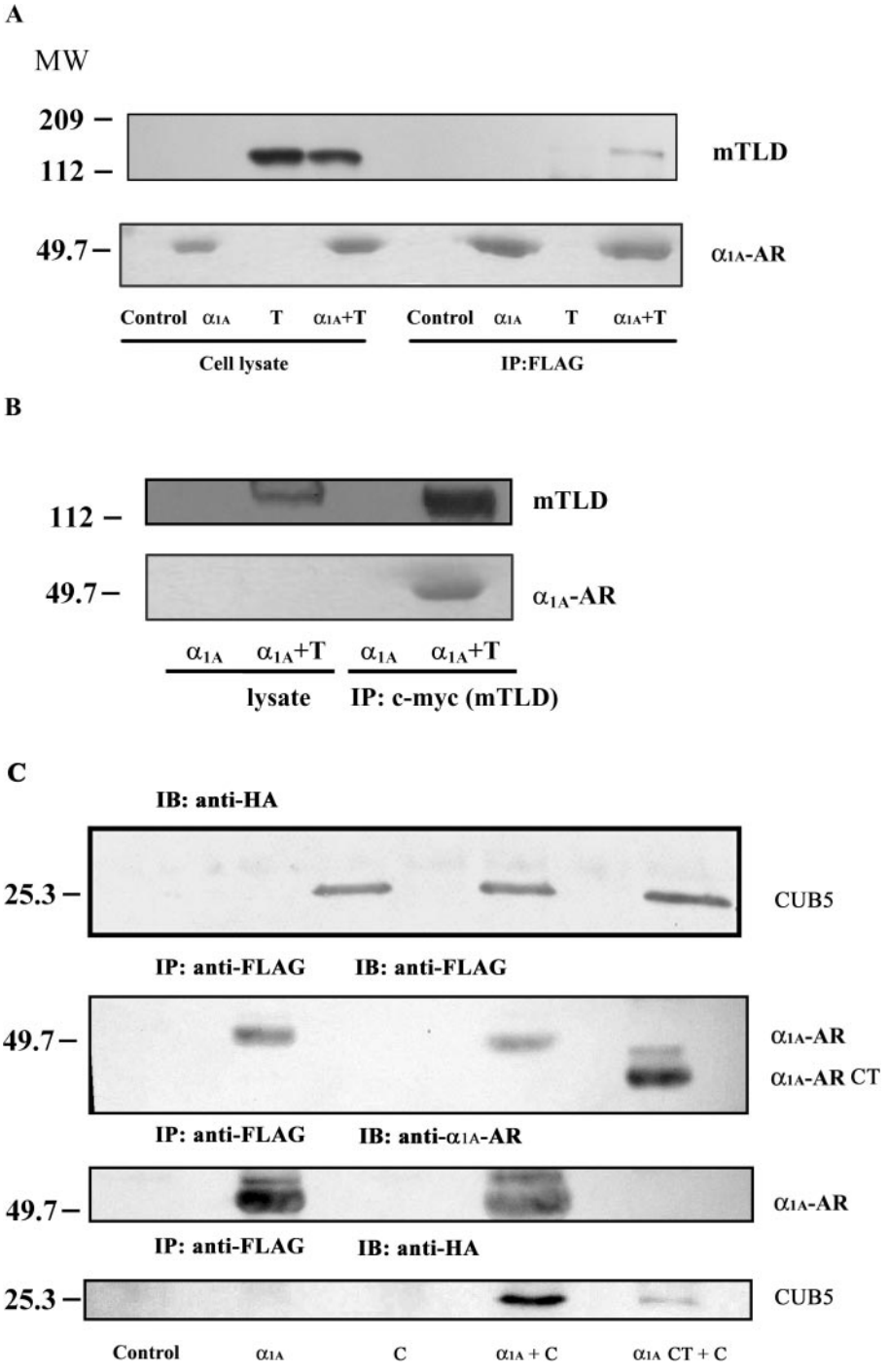

Fig. 4. Binding of mTLD and α_{1A}-AR in transfected HEK293 cells as shown by immunoprecipitation. HEK293 cells transfected with $_{p}$DT-α_{1A} and/or pMT were lysed, and 500 μg of total proteins were immunoprecipitated with anti-FLAG M2 affinity resin (A) or anti-c-myc antibody plus protein-G resin (B). Cell lysates (50 μg) and immunoprecipitates were immunoblotted with anti-mTLD (top) or anti-α_{1A}-AR antibodies (bottom). C, HEK293 cells transfected with $_{p}$DT-α_{1A} or $_{p}$DT-α_{1A}CT and pcP3HA were lysed, and 500 μg of total proteins were immunoprecipitated with anti-FLAG M2 affinity resin. Cell lysates (50 μg, top) and immunoprecipitates (middle and bottom) were immunoblotted with anti-HA, anti-FLAG, or anti-α_{1A}-AR antibodies. Control, nontransfected HEK293 cells; α_{1A}, HEK293 cells transfected with $_{p}$DT-α_{1A}; C, HEK293 cells transfected with pcP3HA; α_{1A} + C, HEK293 cells cotransfected with $_{p}$DT-α_{1A} and pcP3HA; α_{1A}CT+ C, HEK293 cells cotransfected with $_{p}$DT-α_{1A}CT and pcP3HA; T, HEK293 cells transfected with pMT; α_{1A} + T, HEK293 cells cotransfected with $_{p}$DT-α_{1A} and pMT. The results are representative of three independent experiments.

MOL PHARM
MOLECULAR PHARMACOLOGY
aspet

CUB5 domains bound to GST-α_{1A}-AR-cytoplasmic-tail fusion proteins but not to GST alone.

To confirm the interaction between α_{1A}-AR and mTLD in vivo, α_{1A}-AR and mTLD were transiently expressed in HEK293 cells, lysed, and immunoprecipitated by their antibodies, respectively. In immunoblots of cell lysate, bands corresponding to α_{1A}-AR (~50 kDa) and mTLD were revealed by their respective antibodies in transfected but not in untransfected cells (Fig. 4). Immunoprecipitating α_{1A}-AR with anti-Flag M2 affinity resin resulted in coimmunoprecipitation of mTLD, as revealed by the specific ~150-kDa band detected in immunoprecipitates of cotransfected cells. This band was not present in immunoprecipitates from HEK293 cells expressing α_{1A}-AR or mTLD alone. Conversely, reverse immunoprecipitating mTLD also showed coimmunoprecipitation of α_{1A}-AR (Fig. 4). Thus, in HEK293 cells, mTLD interacted specifically with α_{1A}-AR.

Likewise, in HEK293 cells transiently expressing α_{1A}-AR and CUB5 domain, immunoprecipitating α_{1A}-AR with anti-Flag M2 affinity resin also resulted in coimmunoprecipitation of CUB5 (Fig. 4C). Moreover, the CUB5 coimmunoprecipitated by the C-terminally truncated α_{1A}-AR was less than 5% of that by full-length α_{1A}-AR, confirming that the binding to CUB5 domain was mostly contributed by the C terminus of α_{1A}-AR.

Colocalization and Association of HA-Tagged mTLD and α_{1A}-AR. To characterize the mTLD–α_{1A}-AR association in vivo, EGFP-fused α_{1A}-AR and HA-tagged mTLD were transfected into HEK293 cells to allow the subcellular localization of these proteins to be determined using an immunofluorescence assay. As shown in Fig. 5, in cells expressing EGFP-fused α_{1A}-AR alone, fluorescence was observed both on the cell surface and intracellularly (Fig. 5A), which was consistent with previous reports (Chalothorn et al., 2002). When mTLD and α_{1A}-AR were coexpressed, the subcellular localization of α_{1A}-AR was significantly altered. The EGFP fluorescence signal of α_{1A}-AR accumulated predominantly in certain cytoplasmic compartments colocalizing with mTLD

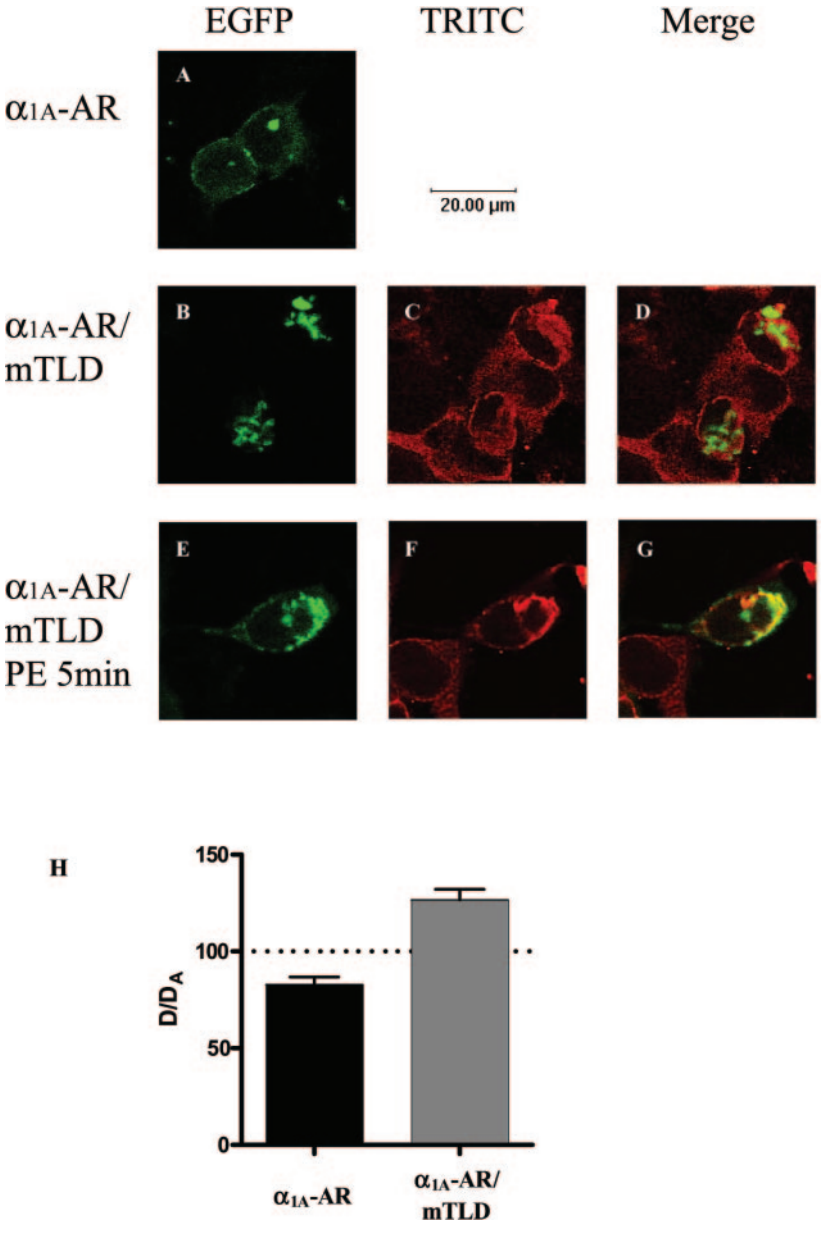

Fig. 5. Colocalization and FRET of α_{1A}-AR and mTLD in transfected HEK293 cells. Images were taken of fixed HEK293 cells using a confocal laser scanning microscope system. A, expressing EGFP-α_{1A}-AR individually; B–D, coexpressing the EGFP-α_{1A}-AR and mTLD/HA; E–G, coexpressing the EGFP-α_{1A}-AR and mTLD/HA, and incubated with 10 μM phenylephrine for 5 min. mTLD was detected using an anti-HA monoclonal antibody and an anti-mouse TRITC-conjugated antibody. Images were taken after excitation at 488 nm for EGFP (A, B, and E) or 543 nm for TRITC (C and F). Merge (D and G) represents the superimposition of the EGFP and TRITC images. Scale bars, 20 μm. The results shown are representative of observations of three independent transfection experiments. H, quantitative analysis of the FRET efficiency. Nine to ten cells from three individual experiments were selected, and the D/D_A value of intracellular areas was averaged.

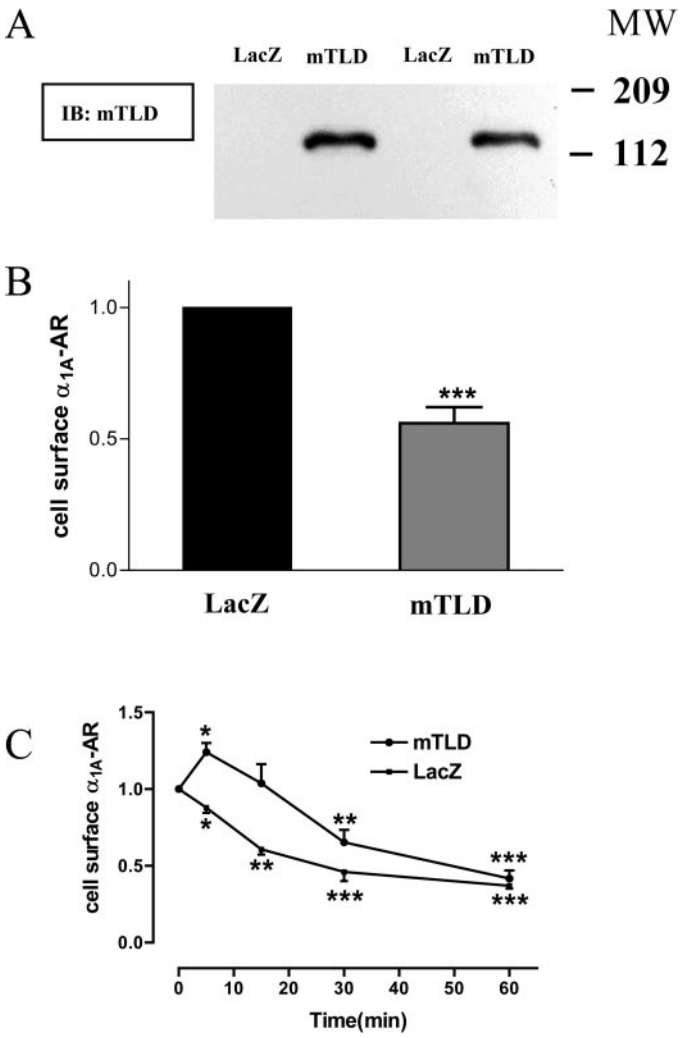

Fig. 6. mTLD changes the number of cell surface α_{1A}-AR and internalization in response to phenylephrine. HEK293 cells expressing α_{1A}-AR were transfected with pcDNA3.1/LacZ or pMT (A). 48 h later, cells were incubated without (B) or with (C) phenylephrine for 5 to 60 min at 37°C. Then transfected cells were fixed, and changes in surface receptor density were subsequently determined by whole-cell ELISA. Data are mean ± S.E. of eight independent experiments, each performed in duplicate and normalized to surface receptor density of control group (B) or untreated cell (C).

(Fig. 5, B, C, and D). However, if the cells were stimulated with 10^{-5} M phenylephrine for 5 min before fixation, colocalization of α_{1A}-AR with mTLD was evident on the cell surface and the cytoplasmic compartment, although the fluorescence signal of α_{1A}-AR was still concentrated in the cytoplasm (Fig. 5, E, F, and G). To validate whether a direct interaction happens between these two molecules, FRET between EGFP-fused α_{1A}-AR (donor fluorescence) and immunofluorescence stained mTLD (acceptor fluorescence) was measured by acceptor photobleaching method. As shown in Fig. 5H, in the absence of mTLD, EGFP signal declined 16.9 ± 3.6% after 5 min of continuous activation of TRITC signal, because EGFP fluorescence could also be excited and inactivated during the process. In the presence of mTLD, however, the fluorescence of the donor in the cells increased 26.7 ± 5.4% after photobleaching of acceptor fluorescence, which indicates a tight intermolecular association between α_{1A}-AR and mTLD in HEK 293 cells.

mTLD Changes The Number of Cell Surface Receptors and the Time Course of Internalization. To verify the finding of subcellular localization of α_{1A}-AR in immunofluorescence assay, we compared the number of cell surface α_{1A}-AR in HEK293 cells stably transfected with $_{P}$DT-α_{1A} in the presence or absence of mTLD (Fig. 6A) using whole-cell ELISA assays. As shown in Fig. 6B, the presence of mTLD reduced the number of cell surface α_{1A}-AR by 44 ± 6% ($P < 0.001$, $n = 8$) compared with cells transfected with a control vector, pcDNA3.1/LacZ. In addition, we examined the time course of α_{1A}-AR internalization in response to phenylephrine (10 μM). As shown in Fig. 6C, in the control group (pcDNA3.1/LacZ transfected), there was a rapid agonist-induced internalization of cell surface receptor with a 63 ± 2% ($n = 8$) reduction after 1 h; in the mTLD group, the time course of α_{1A}-AR internalization was somewhat delayed. The number of cell surface receptors initially increased after 5 min of agonist stimulation and decreased by 58 ± 5% ($n = 8$) between 5 and 60 min of agonist exposure.

mTLD Does Not Alter Density and Affinity of α_{1A}-AR. To study the effect of mTLD on the pharmacological properties of α_{1A}-AR, crude membranes were prepared from HEK293 cells expressing α_{1A}-AR with and without concomitant expression of mTLD. The density and affinity of α_{1A}-AR binding sites were then determined by saturation analysis of

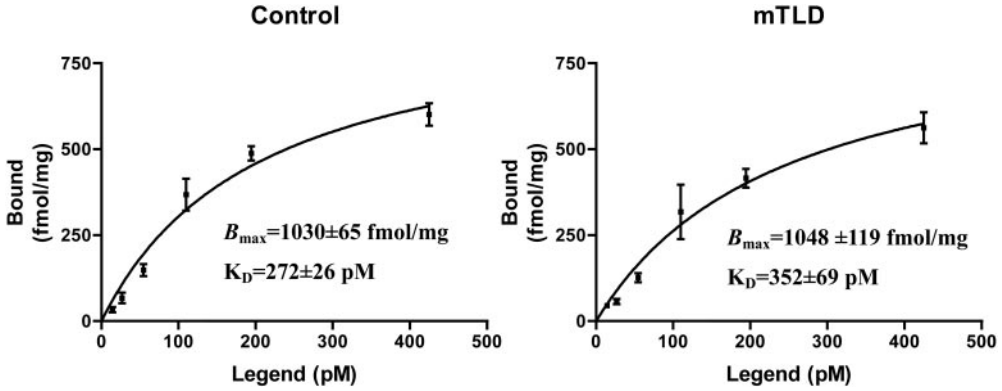

Fig. 7. mTLD does not alter the pharmacological properties of α_{1A}-AR. HEK293 cells expressing α_{1A}-AR were transfected with pcDNA3.1/LacZ or pMT. Membranes were collected 48 h after transfection. Radioligand binding sites were measured by saturation analysis of specific binding of the α_{1A}-AR antagonist radioligand ^{125}I-BE2254 (15–500 pM). Nonspecific binding was defined as binding in the presence of phentolamine (100 μM). Results are the mean ± S.E. of four independent experiments. There was no significant difference in B_{max} and K_D between LacZ-coexpressing and mTLD-coexpressing groups.

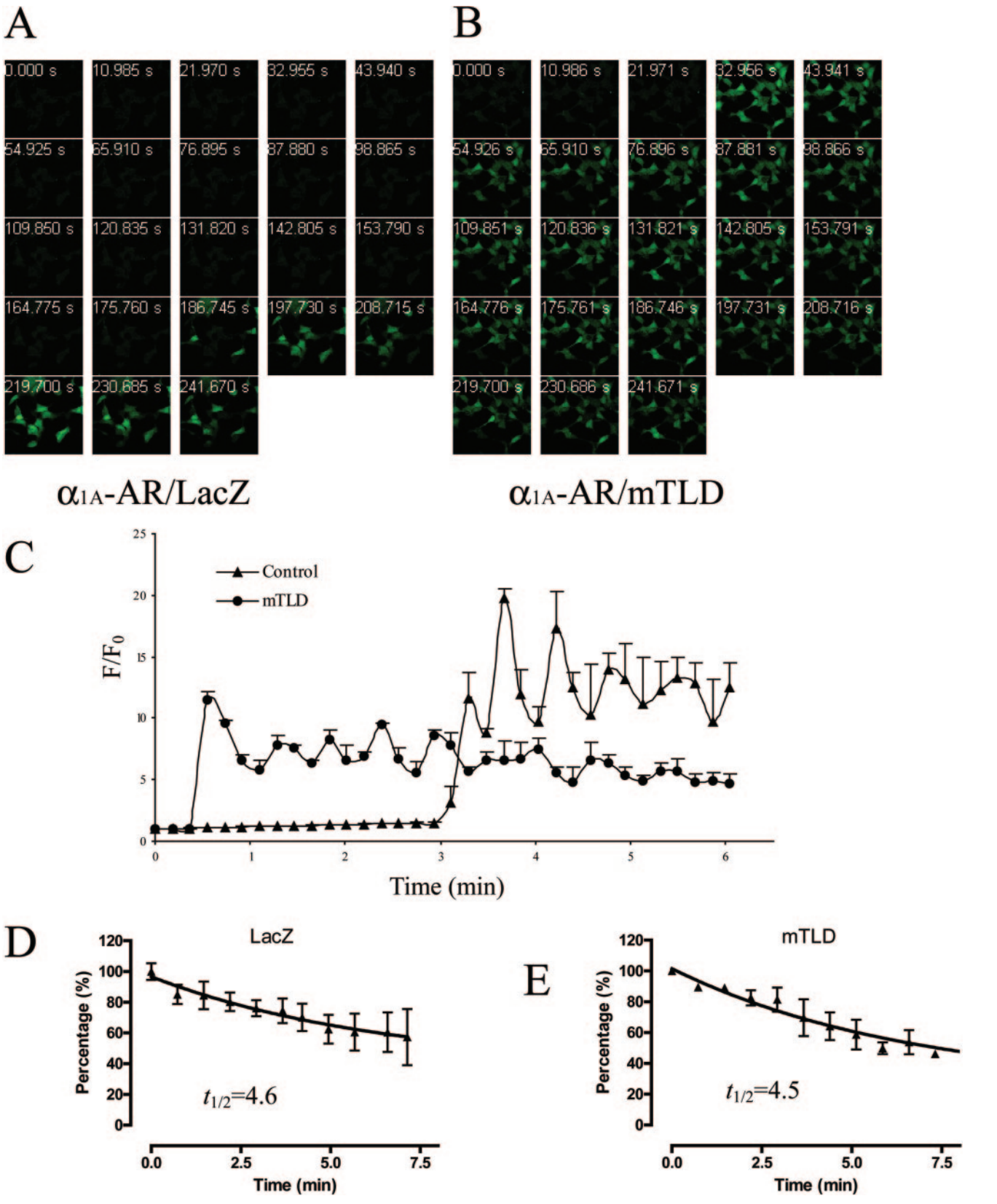

Fig. 8. Time course of intracellular calcium in response to PE stimulation in the presence of LacZ or mTLD. HEK293 cells expressing α_{1A}-AR were transfected with pcDNA3.1/LacZ (A) or pMT (B). Twenty-four hours after transfection, cells were starved with serum-free media for 8 h. Intracellular Ca^{2+} was visualized by confocal microscopy using the calcium indicator fluo-4. Phenylephrine was added to stimulate α_{1A}-AR (final concentration, 10 μM) after three images were acquired. A, a sharp, high-amplitude, and phasic $[Ca^{2+}]_i$ change was observed 2 to 3 min after receptor activation in the control group (LacZ); B, a phasic $[Ca^{2+}]_i$ response occurred immediately after receptor activation in the presence of mTLD; C, quantification of $[Ca^{2+}]_i$ demonstrated that maximum calcium transient of the mTLD group was smaller than control group. D and E, the calcium transient reductions in control and mTLD group display a similar exponential decay with a time constant of 4.5 and 4.6 min, respectively.

the specific binding of the antagonist radioligand ^{125}I-BE2254. As shown in Fig. 7, the presence of mTLD had no effects on the density of α_{1A}-AR. There was no significant difference in B_{max} between LacZ-coexpressing and mTLD-coexpressing groups (1030 ± 65 versus 1048 ± 119 fmol/mg, respectively; both $n = 4$). Furthermore, there was no significant difference in the affinity of α_{1A}-AR to the radioligand ^{125}I-BE2254 in the presence of LacZ or mTLD (272 ± 26 versus 352 ± 69 pM, respectively; both $n = 4$). These results indicated that the interaction of mTLD with α_{1A}-AR does not affect the pharmacological properties of the receptor, although mTLD pulled considerable receptors into intracellular compartment.

Effect of mTLD on Agonist-Induced Changes of Intracellular Calcium Concentration. To further understand the influence of mTLD on α_{1A}-AR signaling function, the dynamics of intracellular calcium concentration ($[Ca^{2+}]_i$) in response to α_{1A}-AR activation was examined with a calcium indicator, fluo-4. In α_{1A}-AR and LacZ cotransfected cells, we detected a sharp, high-amplitude, and phasic $[Ca^{2+}]_i$ change approximately 2 to 3 min after 10 μM phenylephrine stimulation (Fig. 8, A and C). The calcium transient diminished slowly and displayed an exponential decay with a time constant of 4.5 min (Fig. 8D). In contrast to LacZ cotransfected control cells, in the presence of mTLD, the phasic $[Ca^{2+}]_i$ response was initiated immediately after receptor activation. However, the maximum amplitude of the $[Ca^{2+}]_i$ response was relative smaller (Fig. 8, B and C), only approximately 58% of control group, although the attenuation of the calcium transient was also shown as exponential decay with a time constant of 4.6 min (Fig. 8E). We also studied the effect of mTLD on intracellular calcium response to angiotensin-II type 1 receptor (AT1R) and β_1-AR activation. Quantification of $[Ca^{2+}]_i$ demonstrated that in response to β_1-AR activation, intracellular calcium increased slowly, and progressively (Supplemental Data, Fig A). Intracellular calcium in response to AT1R activation occurred immediately after receptor activation (Supplemental Data, Fig B). In both experiments, calcium response was not affected by mTLD.

Discussion

Using techniques for detecting protein-protein interactions, such as protein overlay, yeast two-hybrid assay, phage display, and surface plasmon resonance, increasing numbers of GPCR-associated intracellular partners have been discovered. The intracellular carboxyl terminus cytoplasmic domain is one of the popular regions mediating receptor/non-G protein interactions (Hall et al., 1998; Fraser et al., 2000; Cong et al., 2001). The interactions of GPCRs with various cellular proteins are likely to mediate or regulate the intracellular signaling of receptor, providing explanation for the distinct functions by close-related subtypes within the same family.

However, there are few reports about coupling of α_{1A}-AR with non–G-proteins. In this study, aa 867 to 986 of mTLD, which is located in the CUB5 domain of mTLD (Takahara et al., 1994), was identified as an α_{1A}-AR-interacting protein. We confirmed the interaction of full-length mTLD with α_{1A}-AR in HEK293 cells and showed that the presence of mTLD alters the localization, agonist-induced internalization, and calcium signaling of α_{1A}-AR without affecting its pharmacological properties and intracellular signaling function.

In this study, the ability of the CUB5 domain to bind to two other α_1-AR subtypes was also investigated. Results indicate that the CUB5 domain specifically interacts with the C tail of α_{1A}-AR but not that of α_{1B}- and α_{1D}-AR. This may arise from the poor homology in this region (less than 10%) among the three subtypes (Weinberg et al., 1994). Our results also indicate that a discrete sequence in the cytoplasmic tail of α_{1A}-AR, as demonstrated by the tight binding activity of aa 322 to 359 and halved binding ability of aa 399 to 467, interacted with the CUB5 domain.

So far, the function of the CUB domain remains poorly understood. Some investigators have proposed that CUB domains may be involved in protein-protein interactions (Bond and Beynon, 1995). Recent studies have shed some light on this field; for instance, the CUB1 domain of mTLD was critical for secretion, CUB2 domain was essential for the enzyme activity of the protein (Hartigan et al., 2003), and in the present studies, CUB5 domain was identified to bind to α_{1A}-AR.

Our results demonstrated that α_{1A}-AR not only interacted with the CUB5 domain directly but also associated with full-length mTLD. mTLD, the longer splice variant of BMP-1 (Takahara et al., 1994; Kessler et al., 1996), and BMP-1 share 702 identical amino acids, but mTLD has an additional EGF-like domain and two CUB domains, including the CUB5 domain. To date, most studies on mTLD or BMP-1 have concentrated on identifying their substrates. mTLD (or BMP-1) is able to cleave several precursors of extracellular matrix proteins including procollagens, biglycan, prolysyl oxidase and the chain of laminin-5 (Amano et al., 2000; Scott et al., 2000; Sasaki et al., 2001; Colombo et al., 2003). Little has been known about intracellular function of either mTLD or BMP-1. Only one study showed that intracellular BMP-1 is first synthesized as an inactive pro-BMP-1 and stored in the endoplasmic reticulum and early Golgi compartment (Leighton and Kadler, 2003). Because of the high homology with BMP-1, we hypothesized that mTLD may be processed in a manner similar to that of BMP-1. It is tempting to speculate that mTLD may be synthesized as an inactive form and stored in the endoplasmic reticulum and early Golgi compartments before secretion. Therefore, the intracellular abundance of mTLD made it possible to interact with α_{1A}-AR inside the cells. According to a recent study (Morris et al., 2004), α_{1A}-AR internalizes constitutively, and the surface receptor density is maintained by receptor recycling. This led to speculation that an internal pool of α_{1A}-ARs recycles to allow for continuous agonist-induced signaling. In the same study, this constitutive trafficking was shown to be partially blocked by the Golgi-disturbing agent monensin, implying that the Golgi system is also a potential trafficking system. However, whether mTLD is involved in α_{1A}-AR trafficking through the Golgi system remains unclear.

Using laser-scanning confocal microscopy and whole-cell ELISA, we showed that α_{1A}-AR localized on the cell surface and intracellular compartment in HEK293 cells, an observation consistent with earlier studies (Hirasawa et al., 1997; Chalothorn et al., 2002). In mTLD and α_{1A}-AR cotransfected HEK293 cells, the interaction between α_{1A}-AR and mTLD induced the internalization and accumulation of receptors. Moreover, mTLD influenced the time course of α_{1A}-AR inter-

nalization after agonist exposure. In the absence of mTLD, there was a rapid agonist-induced internalization of cell surface receptor, a finding in agreement with previous studies in HEK293 cells (Chalothorn et al., 2002). In the presence of mTLD, the time course of α_{1A}-AR internalization in response to agonist was different. The number of cell surface receptors initially increased during the first 5 min of agonist stimulation and then decreased by 58% by 60 min. Therefore, the results were consistent with the internalization pattern of α_{1A}-AR in rat-1 fibroblast cells (Price et al., 2002). Price et al. (2002) observed that although the number of cell-surface wild-type α_1-AR showed little increase in the early stages of agonist stimulation, the number of carboxyl-terminally truncated mutant α_1-AR T348 increased significantly during the same period. Given that fibroblasts express mTLD naturally, whereas there was no mTLD expression at the mRNA level in HEK293 cells (data not shown), and considering our results that amino acid residues 322 to 359 are the primary binding region to CUB5 domain of mTLD, conflicting results of α_{1A}-AR internalization from different groups are expected. The naturally expressed mTLD participates in the internalization of α_{1A}-AR in fibroblasts, similar to what we observed in mTLD-transfected HEK293 cells. Partial deletion of the receptor's cytoplasmic tail would expose the primary binding region and tighten the interaction of mTLD and α_{1A}-AR, thereby enhancing the influence of mTLD on the localization of α_{1A}-AR.

On the other hand, phosphorylation, desensitization, internalization, and down-regulation of the receptor in response to agonist exposure would occur within seconds to hours after stimulation. Whereas arrestins have been implicated in mediating the internalization of a variety of GPCRs, the effects of β-arrestin on α_{1A}-AR are not clear. gC1q-R is a cellular protein that interacts with α_{1B}- and α_{1D}-AR, and regulates the cellular localization and expression of α_{1B}-AR. Thus, it is interesting that mTLD expression alters the subcellular localization and internalization of α_{1A}-AR as shown in the present study.

Our results suggest that mTLD did not alter the density or affinity of α_{1A}-AR, although it altered the subcellular localization of the receptor. Thus, receptor internalization does not alter the conformation of α_{1A}-AR, or at least does not alter the conformation of the ligand-binding region. It has been reported that α_{1D}-ARs mainly localize intracellularly in a perinuclear orientation (Chalothorn et al., 2002) and that this fraction of the receptors can still respond well to agonist stimulation (McCune et al., 2000; Waldrop et al., 2002). Therefore, it is possible that internalized α_{1A}-AR is still localized in certain intracellular membrane structures and preserves the receptor structure and ligand binding properties.

We observed an enhanced intracellular calcium response to α_{1A}-AR activation in the presence of mTLD, although the time course of calcium transient decay was not altered. In addition, the effect of mTLD on intracellular calcium response to α_{1A}-AR activation was not observed on two other GPCRs, AT1R and β_1-AR. Although the physiological mechanism of calcium signaling flux remains to be investigated, it seems clear that mTLD plays an important role in the early response of α_{1A}-AR to agonist by ensuring a rapid reaction after receptor activation.

In conclusion, we have demonstrated that mTLD is a novel and specific intracellular partner of α_{1A}-AR, and the interaction of these two proteins influences the localization, internalization, and calcium signaling function of α_{1A}-AR. The precise mechanism of mTLD's effects on α_{1A}-AR is an important target for further investigation.

Acknowledgments

We thank Prof. K. P. Minneman for the generous gift of α_1-AR cDNAs. We also thank Prof. K. P. Minneman and Dr. Xiaojun Du (Baker Heart Research Institute, Melbourne, Australia) for review and advice on this article.

References

Amano S, Scott IC, Takahara K, Koch M, Champliaud MF, Gerecke DR, Keene DR, Hudson DL, Nishiyama T, Lee S, et al. (2000) Bone morphogenetic protein 1 is an extracellular processing enzyme of the laminin 5 γ2 chain. *J Biol Chem* **275:** 22728–22735.

Autelitano DJ and Woodcock EA (1998) Selective activation of alpha1A-adrenergic receptors in neonatal cardiac myocytes is sufficient to cause hypertrophy and differential regulation of alpha1-adrenergic receptor subtype mRNAs. *J Mol Cell Cardiol* **30:**1515–1523.

Bond JS and Beynon RJ (1995) The astacin family of metalloendopeptidases. *Protein Sci* **4:**1247–1261.

Brzostowski JA and Kimmel AR (2001) Signaling at zero G: G-protein-independent functions for 7-TM receptors. *Trends Biochem Sci* **26:**291–297.

Chalothorn D, McCune DF, Edelmann SE, Garcia-Cazarin ML, Tsujimoto G, and Piascik MT (2002) Differences in the cellular localization and agonist-mediated internalization properties of the α_1-adrenoceptor subtypes. *Mol Pharmacol* **61:** 1008–1016.

Chen S, Lin F, Iismaa S, Lee KN, Birckbichler PJ, and Graham RM (1996) Alpha1-adrenergic receptor signaling via Gh is subtype specific and independent of its transglutaminase activity. *J Biol Chem* **271:**32385–32391.

Colombo M, Brittingham RJ, Klement JF, Majsterek I, Birk DE, Uitto J, and Fertala A (2003) Procollagen VII self-assembly depends on site-specific interactions and is promoted by cleavage of the NC2 domain with procollagen C-proteinase. *Biochemistry* **42:**11434–11442.

Cong M, Perry SJ, Lin FT, Fraser ID, Hu LA, Chen W, Pitcher JA, Scott JD, and Lefkowitz RJ (2001) Regulation of membrane targeting of the G protein-coupled receptor kinase 2 by protein kinase A and its anchoring protein AKAP79. *J Biol Chem* **276:**15192–15199.

Diviani D, Lattion AL, Abuin L, Staub O, and Cotecchia S (2003) The adaptor complex 2 directly interacts with the α_{1b}-adrenergic receptor and plays a role in receptor endocytosis. *J Biol Chem* **278:**19331–19340.

Fraser ID, Cong M, Kim J, Rollins EN, Daaka Y, Lefkowitz RJ, and Scott JD (2000) Assembly of an A kinase-anchoring protein-β_2-adrenergic receptor complex facilitates receptor phosphorylation and signaling. *Curr Biol* **10:**409–412.

Grupp IL, Lorenz JN, Walsh RA, Boivin GP, and Rindt H (1998) Overexpression of alpha1B-adrenergic receptor induces left ventricular dysfunction in the absence of hypertrophy. *Am J Physiol* **275:**H1338–H1350.

Hall RA, Premont RT, Chow CW, Blitzer JT, Pitcher JA, Claing A, Stoffel RH, Barak LS, Shenolikar S, Weinman EJ, et al. (1998) The beta2-adrenergic receptor interacts with the Na^+/H^+-exchanger regulatory factor to control Na^+/H^+ exchange. *Nature (Lond)* **392:**626–630.

Hall RA, Premont RT, and Lefkowitz RJ (1999) Heptahelical receptor signaling: beyond the G protein paradigm. *J Cell Biol* **145:**927–932.

Hartigan N, Garrigue-Antar L, and Kadler KE (2003) Bone morphogenetic protein-1 (BMP-1). Identification of the minimal domain structure for procollagen C-proteinase activity. *J Biol Chem* **278:**18045–18049.

Heuss C and Gerber U (2000) G-protein-independent signaling by G-protein-coupled receptors. *Trends Neurosci* **23:**469–475.

Hirasawa A, Sugawara T, Awaji T, Tsumaya K, Ito H, and Tsujimoto G (1997) Subtype-specific differences in subcellular localization of alpha1-adrenoceptors: chlorethylclonidine preferentially alkylates the accessible cell surface α1-adrenoceptors irrespective of the subtype. *Mol Pharmacol* **52:**764–770.

Kessler E, Takahara K, Biniaminov L, Brusel M, and Greenspan DS (1996) Bone morphogenetic protein-1: the type I procollagen C-proteinase. *Science (Wash DC)* **271:**360–362.

Klein U, Ramirez MT, Kobilka BK, and von Zastrow M (1997) A novel interaction between adrenergic receptors and the alpha-subunit of eukaryotic initiation factor 2B. *J Biol Chem* **272:**19099–19102.

Leighton M and Kadler KE (2003) Paired basic/Furin-like proprotein convertase cleavage of Pro-BMP-1 in the trans-Golgi network. *J Biol Chem* **278:**18478–18484.

McCune DF, Edelmann SE, Olges JR, Post GR, Waldrop BA, Waugh DJ, Perez DM, and Piascik MT (2000) Regulation of the cellular localization and signaling properties of the α_{1B}- and α_{1D}-adrenoceptors by agonists and inverse agonists. *Mol Pharmacol* **57:**659–666.

Menard L, Ferguson SS, Zhang J, Lin FT, Lefkowitz RJ, Caron MG, and Barak LS (1997) Synergistic regulation of β_2-adrenergic receptor sequestration: intracellular complement of β-adrenergic receptor kinase and β-arrestin determine kinetics of internalization. *Mol Pharmacol* **51:**800–808.

Morris DP, Price RR, Smith MP, Lei B, and Schwinn DA (2004) Cellular trafficking of human α_{1a}-adrenergic receptors is continuous and primarily agonist-independent. *Mol Pharmacol* **66:**843–854.

Price RR, Morris DP, Biswas G, Smith MP, and Schwinn DA (2002) Acute agonist-mediated desensitization of the human α_{1a}-adrenergic receptor is primarily inde-

pendent of carboxyl terminus regulation: implications for regulation of alpha 1aAR splice variants. *J Biol Chem* **277:**9570–9579.
Pupo AS and Minneman KP (2002) Interaction of neuronal nitric oxide synthase with alpha1-adrenergic receptor subtypes in transfected HEK-293 cells. *BMC Pharmacol* **2:**17.
Pupo AS and Minneman KP (2003) Specific interactions between gC1qR and alpha1-adrenoceptor subtypes. *J Recept Signal Transduct Res* **23:**185–195.
Sasaki T, Gohring W, Mann K, Brakebusch C, Yamada Y, Fassler R, and Timpl R (2001) Short arm region of laminin-5 gamma2 chain: structure, mechanism of processing and binding to heparin and proteins. *J Mol Biol* **314:**751–763.
Scott IC, Imamura Y, Pappano WN, Troedel JM, Recklies AD, Roughley PJ, and Greenspan DS (2000) Bone morphogenetic protein-1 processes probiglycan. *J Biol Chem* **275:**30504–30511.
Takahara K, Lyons GE, and Greenspan DS (1994) Bone morphogenetic protein-1 and a mammalian tolloid homologue (mTld) are encoded by alternatively spliced transcripts which are differentially expressed in some tissues. *J Biol Chem* **269:**32572–32578.
Vazquez-Prado J, Medina LC, Romero-Avila MT, Gonzalez-Espinosa C, and Garcia-Sainz JA (2000) Norepinephrine- and phorbol ester-induced phosphorylation of α_{1a}-adrenergic receptors. Functional aspects. *J Biol Chem* **275:**6553–6559.
Waldrop BA, Mastalerz D, Piascik MT, and Post GR (2002) α_{1B}- and α_{1D}-Adrenergic receptors exhibit different requirements for agonist and mitogen-activated protein kinase activation to regulate growth responses in rat 1 fibroblasts. *J Pharmacol Exp Ther* **300:**83–90.
Wang SQ, Song LS, Lakatta EG, and Cheng H (2001) Ca^{2+} signalling between single L-type Ca^{2+} channels and ryanodine receptors in heart cells. *Nature (Lond)* **410:**592–596.
Weinberg DH, Trivedi P, Tan CP, Mitra S, Perkins-Barrow A, Borkowski D, Strader CD, and Bayne M (1994) Cloning, expression and characterization of human alpha adrenergic receptors alpha 1a, alpha 1b and alpha 1c. *Biochem Biophys Res Commun* **201:**1296–1304.
Xu Q, Zhang T, Han QD, and Zhang YY (2003) Binding between alpha 1A-adrenergic receptor and segment of bone morphogenetic protein-1 in human embryonic cell 293. *Sheng Li Xue Bao* **55:**692–698.
Zhong H, Lee D, Robeva A, and Minneman KP (2001) Signaling pathways activated by alpha1-adrenergic receptor subtypes in PC12 cells. *Life Sci* **68:**2269–2276.
Zhong H and Minneman KP (1999) Differential activation of mitogen-activated protein kinase pathways in PC12 cells by closely related alpha1-adrenergic receptor subtypes. *J Neurochem* **72:**2388–2396.
Zhu W, Zhang Y, and Han C (1997) Characterization of subtype of alpha1-adrenoceptor mediating vasoconstriction in perfused rat hind limb. *Eur J Pharmacol* **329:**55–61.

Address correspondence to: Youyi Zhang, Institute of Vascular Medicine, Peking University Third Hospital, No.49 Huayuan North Road, Haidian District, Beijing, P.R. China 100083. E-mail: zhangyy@bjmu.edu.cn